3D photoluminescent Eu(III)-MOF sensor supported by tetracarboxylate ligand for the sensitive and selective detection of Cd^{2+} and *o*-nitrophenol

CharanjeetSen,[a] SwaitaDevi,[a] Niharika,[a] NidhiBhagat,[a] Haq Nawaz Sheikh[a,*]

[a]Department of Chemistry, University of Jammu, Baba Sahib Ambedkar Road, Jammu 180006, India

Table of Contents

CONTENTS

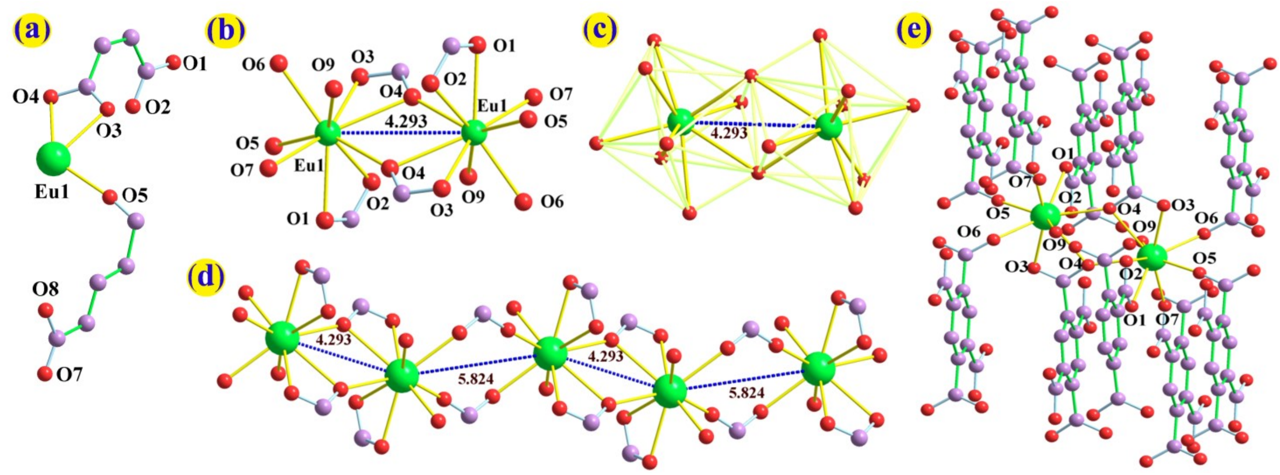

Figure S1:(a) Asymmetric unit of **Cj-2**; (b) SBU of**Cj-2** (Eu…Eu = 4.293); (c) Edge sharing in SBU; (d) Linear extension of dinuclear SBUs; (e) The dinuclear unit connected with ten BTA ligands in **Cj-2**.

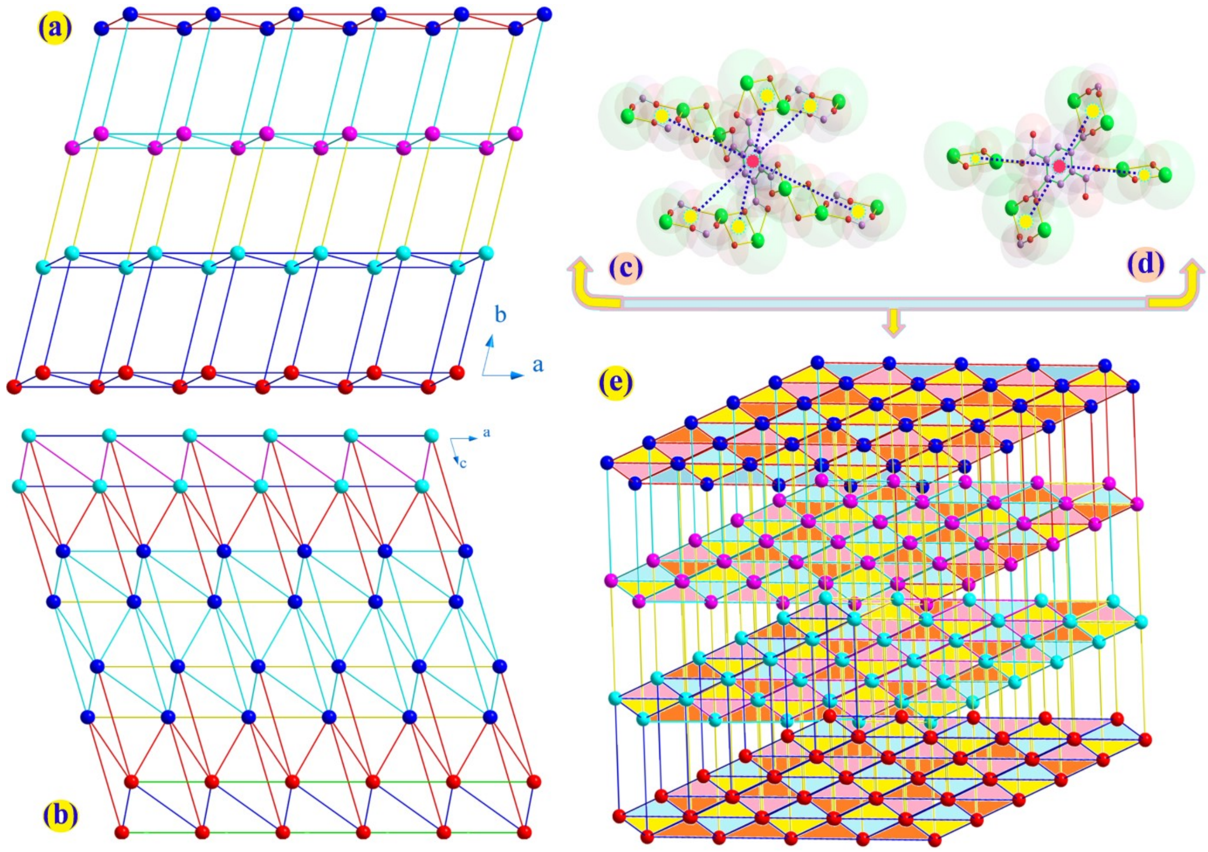

Figure S2:2D representation of (4,4) rtectangular grid array nurturing by connecting Eu(III) nodes along the (a) ab and (b) ac plane; (c) Each BTA^{4-} linking six dinuclear SBUs, forming a 6-connected node (d) Each H_2BTA^{2-}linking four dinuclearEu (III) SBUs unit is defined as a 4-connected node (e) Topogical diagram of **Cj-2**.

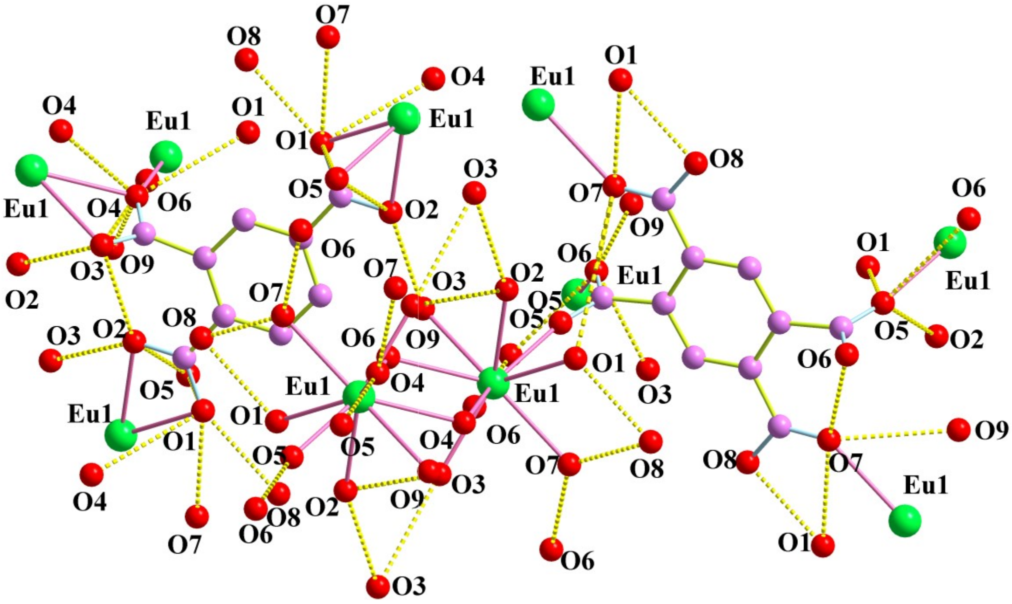

Figure S3: Hydrogen bonding positions in **Cj-2**

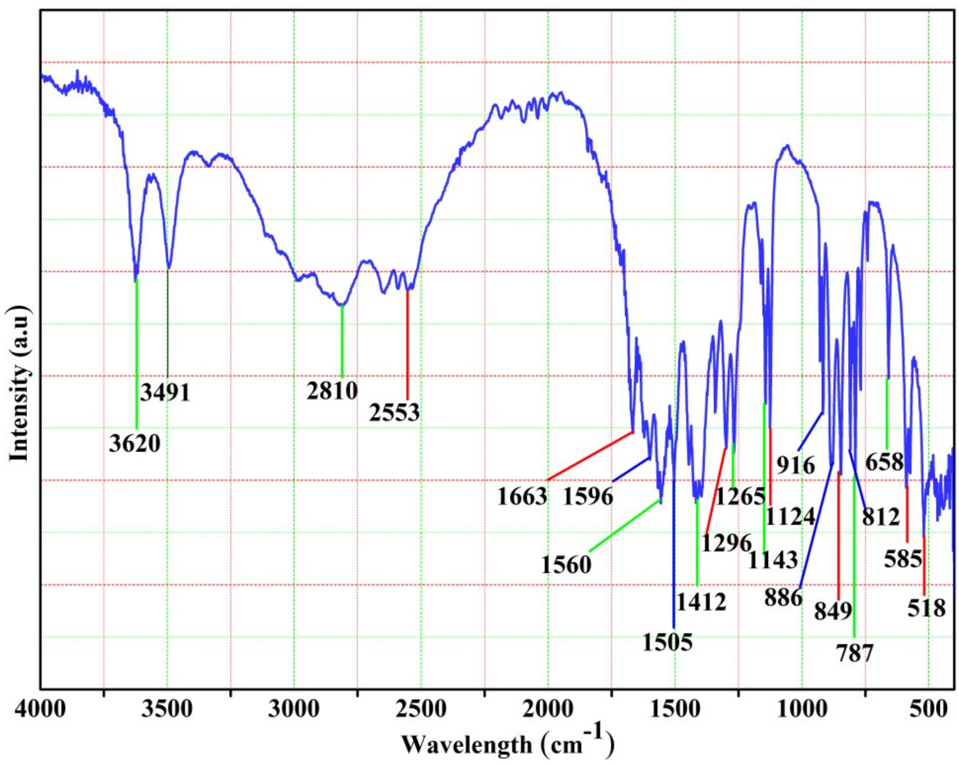

Figure S4:FTIR spectrum of **Cj-2**.

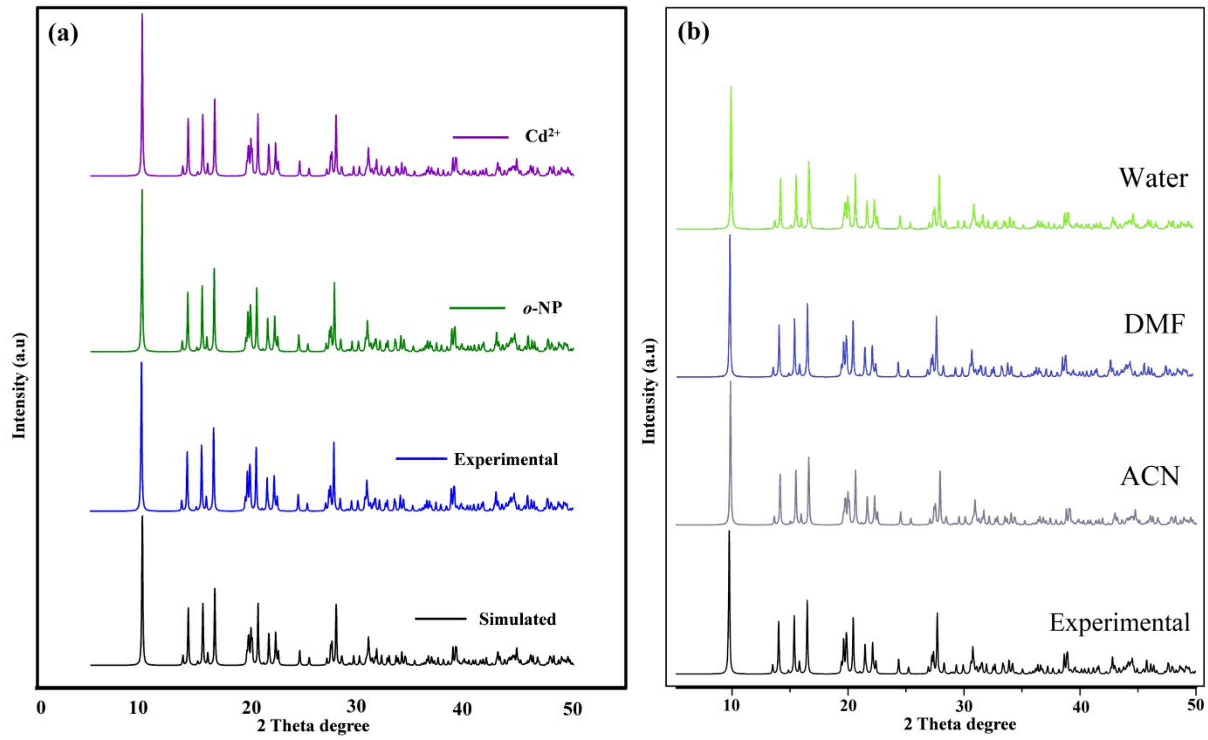

Figure S5. (a) Experimental and simulated PXRD Patterns of **Cj-2,** along with the PXRD response of recycled **Cj-2** after addition of *o*-NP, andCd^{2+}. (b) Experimental PXRD Patterns of **Cj-2,** along with the PXRD response of **Cj-2** in water, DMF and ACN.

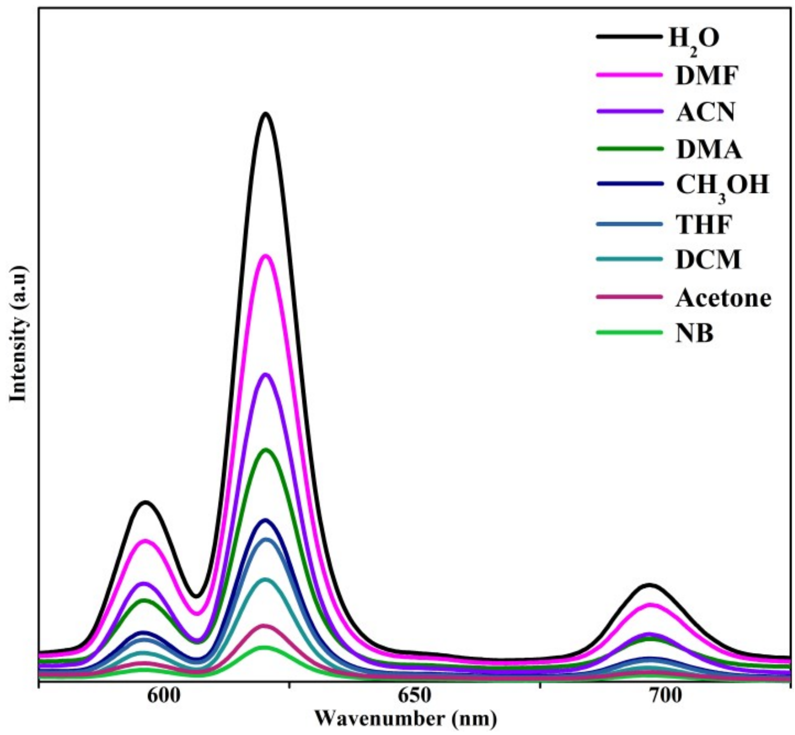

Figure S6. Emission spectra of **Cj-2** in different solvents.

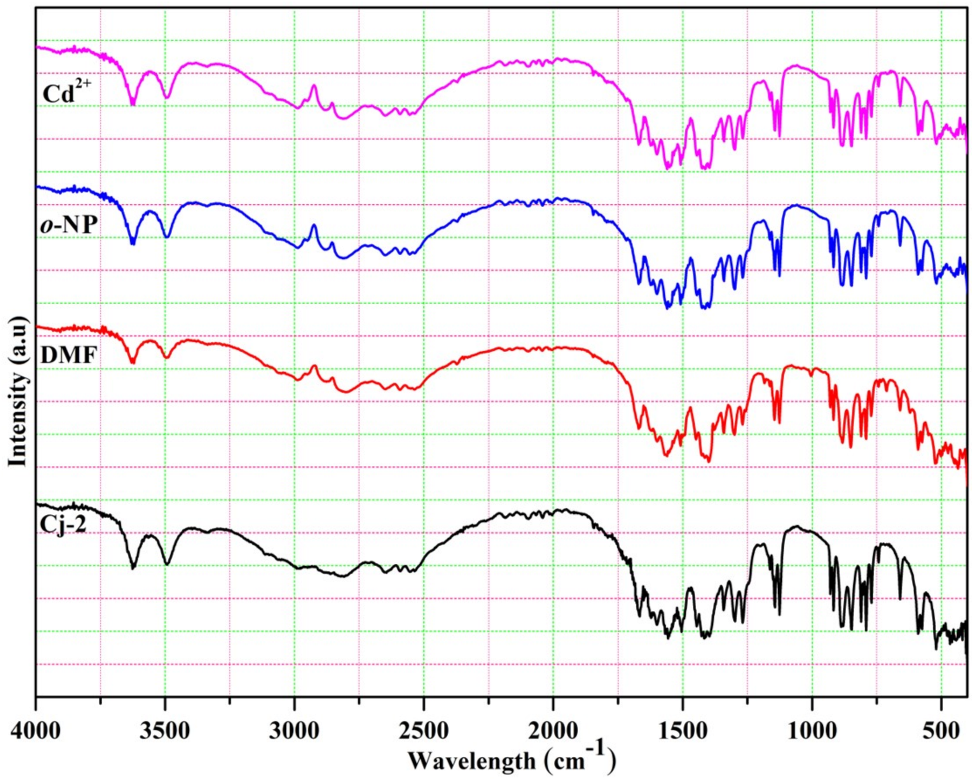

Figure S7. IR spectra of recycled **Cj-2** after addition of *o*-NP, andCd^{2+}.

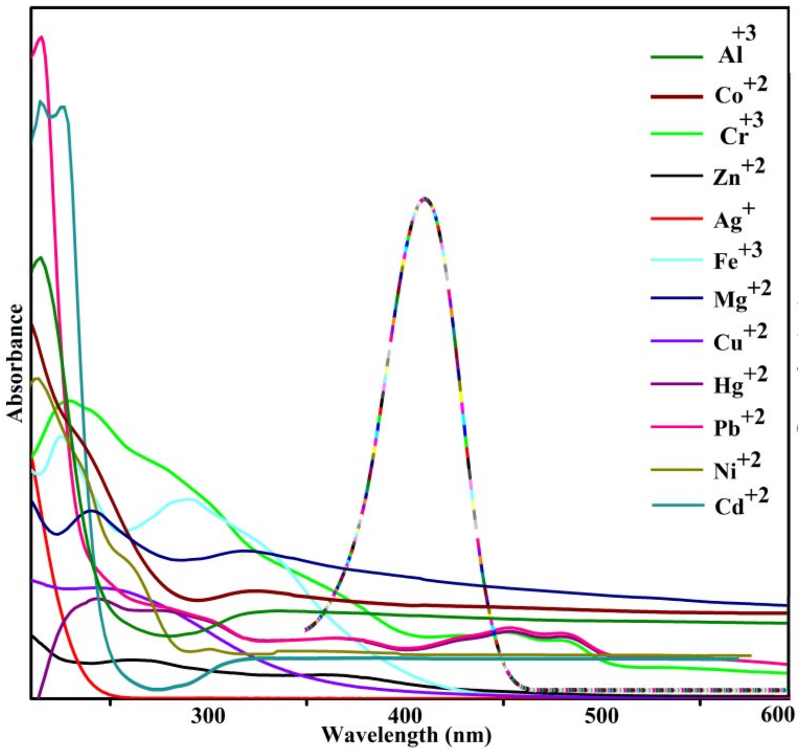

Figure S8. UV-Vis Absorption spectra of metals ions.

Thermogravimetric Analysis

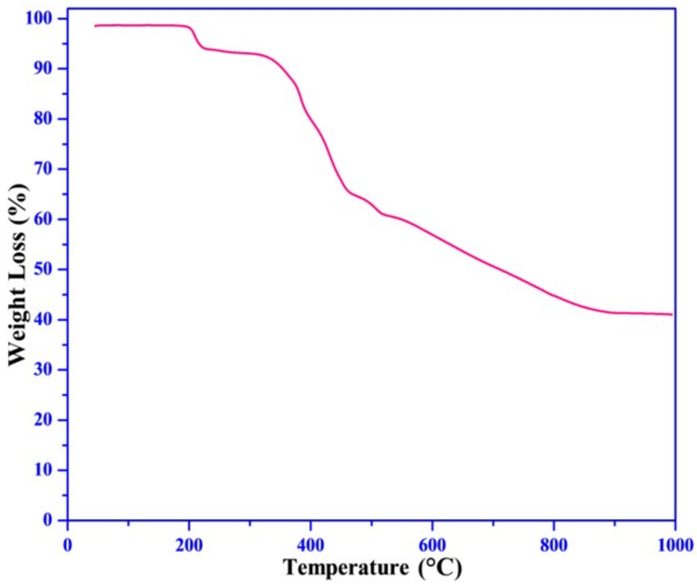

Figure S9: Thermogravimetric analysis curve of Cj-2.

The thermal decomposition behavior of synthesized Cj-2 was investigated using thermogravimetric analysis under an inert atmosphere (N_2 gas), with a heating rate of 10 °C/min from 30 to 950 °C. Cj-2 demonstrates thermal stability up to 190 °C. Above this temperature, it undergoes two successive weight loss events between 190 and 960 °C. In the first stage, there is a 4.27% weight loss observed from 190 to 270 °C, attributed to the removal of coordinated water molecules (calculated at 4.60%). The second decomposition stage begins at 320 °C and continues without a distinct endpoint within the limits of the thermal analyzer. This stage begins with a sudden weight loss followed by a gradual decline, possibly due to the structural collapse and oxidation of the organic linker (BTA). At 690 °C, the decomposition process results in the formation of Eu_2O_3, which remains stable up to 950 °C.

Table S1: Crystal data for Cj-2

Crystallographic Information (Tables)

Empirical formula	**$C_{10}H_5EuO_9$**
CCDC	**2356125**
Formula weight	**421.10**
Crystal system	**Triclinic**
space group	***P*–1**
Temperature (K)	**200(2) K**
***a*(Å)**	**6.3270(7)**
***b*(Å)**	**9.2759(10)**
***c*(Å)**	**9.4488(10)**
α(deg°)	**88.275(5)°**
β (deg °)	**73.972(5)°**
γ (deg °	**76.714(5)°**
***V*olume (Å^3)**	**518.39(10) Å^3**
Z	**2**
Radiation type	**Cu Kα (λ =1.54178 Å)**
μ (mm^{-1})	**43.843**
Crystal size (mm^3)	**0.200 × 0.180 × 0.150 mm^3**
T_{min}, T_{max}	**0.017, 0.116**
No. of reflections	**1810**
R_{int}	**0.0568**
(sin θ/λ)$_{max}$ (Å^{-1})	**0.648**
$R[F^2 > 2\sigma(F^2)]$, $wR(F^2)$, S	**0.0327, 0.0875, 0.0887**
No. of reflections	**75738**
No. of parameters	**190**
$\Delta\rho_{max}$, $\Delta\rho_{min}$ (e Å^{-3})	**1.031, −0.894**
Goodness-of-fit on F^2	**1.129**

Table S2: Hydrogen-bond geometry (Å, °) for Cj-2

Type	Donor-H....Acceptor	D - H	H...A	D...A	D - H...A
	O8-H8A...O1^{i}	0.84	1.73	2.549(6)	164
	O9-H9A...O2^{ii}	0.85(7)	2.14(8)	2.891(6)	147(7)
	O9-H9A...O3^{ii}	0.85(7)	2.31(8)	2.872(7)	124(6)
Intra	O9-H9A...O2^{iii}	0.85(7)	2.59(8)	3.087(7)	118(7
	O9-H9B...O3^{ii}	0.87(10)	2.54(13)	2.872(7)	104(9)
Intra	C4-H4...O1^{iv}	0.95	2.46	2.782(7)	100
Intra	C8-H8...O8	0.95	2.31	2.677(8)	102
Intra	C8-H8...O3^{v}	0.95	2.59	3.156(7)	118'

Symmetry code(s): (i) -1+x,1+y,-1+z (ii) -1+x,y,z (iii) -x,1-y,2-z (iv) 1-x,-y,2-z (v) 1-x,-y, 2-z

Table S3: Selected geometric parameters (Å) for Cj-2

Eu1—O5	2.325 (4)	Eu1—O1^{iii}	2.480 (4)
Eu1—O9	2.380 (5)	Eu1—O7^{iv}	2.488 (4)
Eu1—O6^{i}	2.380 (4)	Eu1—O2^{iii}	2.531 (4)
Eu1—O3	2.446 (4)	Eu1—O4	2.563 (4)
Eu1—O4^{ii}	2.454 (4)	Eu1—Eu1^{ii}	4.2927 (6)

Symmetry code(s): (i) −*x*+1, −*y*+1, −*z*+1; (ii) −*x*, −*y*+1, −*z*+2; (iii) −*x*+1, −*y*+1, −*z*+2; (iv) −*x*, −*y*+2, −*z*+1.

Table S4: Selected geometric parameters (°) for Cj-2

O5—Eu1—O9	139.63 (16)	O3—Eu1—O7^{iv}	157.70 (14)
O5—Eu1—O6^{i}	76.49 (14)	O4^{ii}—Eu1—O7^{iv}	86.82 (14)
O9—Eu1—O6^{i}	66.78 (15)	O1^{iii}—Eu1—O7^{iv}	71.13 (14)

O5—Eu1—O3	**80.95 (14)**	**O5—Eu1—O2^{iii}**	**73.50 (14)**
O9—Eu1—O3	**102.58 (17)**	**O9—Eu1—O2^{iii}**	**146.45 (14)**
O6^{i}—Eu1—O3	**72.59 (14)**	**O6^{i}—Eu1—O2^{iii}**	**137.00 (13)**
O5—Eu1—O4^{ii}	**145.62 (14)**	**O3—Eu1—O2^{iii}**	**72.86 (13)**
O9—Eu1—O4^{ii}	**70.42 (15)**	**O4^{ii}—Eu1—O2^{iii}**	**80.73 (13)**
O6^{i}—Eu1—O4^{ii}	**136.89 (13)**	**O1^{iii}—Eu1—O2^{iii}**	**51.66 (13)**
O3—Eu1—O4^{ii}	**112.92 (13)**	**O7^{iv}—Eu1—O2^{iii}**	**122.68 (13)**
O5—Eu1—O1^{iii}	**73.14 (14)**	**O5—Eu1—O4**	**128.75 (14)**
O9—Eu1—O1^{iii}	**129.70 (17)**	**O9—Eu1—O4**	**76.89 (16)**
O6^{i}—Eu1—O1^{iii}	**142.12 (14)**	**O6^{i}—Eu1—O4**	**102.25 (13)**
O3—Eu1—O1^{iii}	**123.14 (13)**	**O3—Eu1—O4**	**51.59 (12)**
O4^{ii}—Eu1—O1^{iii}	**73.08 (13)**	**O4^{ii}—Eu1—O4**	**62.37 (15)**
O5—Eu1—O7^{iv}	**88.28 (15)**	**O1^{iii}—Eu1—O4**	**114.30 (13)**
O9—Eu1—O7^{iv}	**73.42 (17)**	**O7^{iv}—Eu1—O4**	**142.95 (14)**
O6^{i}—Eu1—O7^{iv}	**85.97 (14)**	**O2^{iii}—Eu1—O4**	**74.72 (13)**

Symmetry code(s): (i) −*x*+1, −*y*+1, −*z*+1; (ii) −*x*, −*y*+1, −*z*+2; (iii) −*x*+1, −*y*+1, −*z*+2; (iv) −*x*, −*y*+2, −*z*+1.